

Acid Neutralization Capacity of Metakaolin-based Geopolymers

Neven Ukrainczyk¹ | Eddie Koenders¹

Correspondence

Dr. Neven Ukrainczyk
TU Darmstadt, Institute of Construction and Building Materials,
Franziska Braun-Straße 3,
64287 Darmstadt, Germany
Email: ukrainczyk@wib.tu-darmstadt.de

¹Institute of Construction and Building Materials, Technical University of Darmstadt, Germany

Abstract

A titration method is used to analyse the acid neutralization/consumption capacity (ANC) of cement binders, which involves plotting the steady-state pH against the amount of acid added to a diluted suspension of hardened cement samples. Despite ANC being employed for several decades, there is no reported application of ANC for metakaolin-based geopolymers. This study compares the resistance of metakaolin geopolymers to acetic acid and hydrochloric acid with that of Calcium Aluminate Cement (CAC) and Portland Cement (PC). The proposed ANC test setup involves small acid dosage steps using an auto-titrator, resulting in a high-resolution titration curve. The effect of binder chemical composition on acid resistance is evaluated through cumulative and differential ANC analysis, providing a new rapid approach to evaluate the durability of geopolymers in low pH environments.

Keywords

Acid neutralisation capacity, Geopolymers, Metakaolin, Calcium Aluminate Cement, Portland Cement, Acid Attack.

1 Introduction

Concrete design for acidic conditions is categorized into exposure classes (XA1, XA2, or XA3) based on aggressive species concentrations, including pH [1]. Surface protection methods such as coatings and linings are commonly required to mitigate these effects. However, polymer coatings/linings can face durability challenges. Calcium aluminate cements offer a viable alternative to Portland-based cements, delivering improved performance in various environments and accelerated lab tests, despite higher initial costs. Additionally, alkali activated materials, such as geopolymers, are emerging as promising alternatives with enhanced durability, sustainability, and environmental friendliness. Ukrainczyk [1] investigated the interplay between metakaolin composition, geopolymer design parameters, and alkali leaching in acetic acid, highlighting the influence of geopolymerization reaction on alkali ion binding capacity.

The Acid Neutralization Capacity (ANC) is a valuable parameter used to assess neutralization capacity [2-5]. It measures the amount of acid (mmol) required to dissolve 1 g of a specific substance. ANC is determined by constructing a titration curve, plotting the steady state pH against the amount of acid added to ground samples. This quantitative measure helps compare the neutralization effectiveness of different materials. While the ANC of cement binders has been extensively studied, its application in geopolymers is a novel and unexplored research area.

The titration experiments conducted in this study offer a time-efficient method for investigating neutralization capacity. Unlike longer-duration approaches, the titration method provides results in just a few hours or up to a day, making it a valuable tool for obtaining an initial understanding of the neutralization behavior of different substances. While longer-duration methods may offer greater accuracy, the titration method serves as a practical and efficient approach in comparing the neutralization behaviour of different binder types. The Acid Neutralization Capacity method (ANC) is a widely recognized engineering parameter extensively used in various fields such as solidified wastes, radioactive wastes, and heavy metals characterization [2, 3]. The determination of ANC for cementitious materials has become a common quantitative analytical technique [4]. It is well-known that Portland cement exhibits high pH and ANC values. However, when pozzolanic binders are incorporated to partially replace Portland cement, the ANC decreases due to the altered chemical composition of the hydrated specimens [2]. Recently, Damion and Chaunsali (2022) [6] investigated the effect of chemical composition on acid resistance using citric and sulfuric acid, as evaluated by ANC, presenting a novel approach to assess the durability of CSA and CAC cements. In a study by Mellado et al. (2017) [7], the resistance of alkali-activated pastes, prepared from ground granulated blast slag, fly ash, spent catalyst, and ceramic waste, to nitric acid attack was investigated in comparison to hardened Portland cement pastes. Unlike our current

study, ANC measurements were conducted at controlled pH values of 2, 4, and 7. Despite ANC being employed for several decades, there are no reported applications of ANC for metakaolin-based geopolymers. Geopolymers are inorganic binders with low calcium content that offer strong resistance to organic and mineral acids in concrete structures. A low calcium content in geopolymers represents a vital feature [8] and separates them from a broader class of alkali-activated binders.

This paper addresses the research gaps in the existing literature by comparing the ANC of metakaolin geopolymers with that of Calcium Aluminate Cement (CAC) and Portland Cement (PC) under acetic acid and hydrochloric acid attack. Our proposed ANC test setup involves incremental acid dosages using an auto-titrator, resulting in a high-resolution titration curve. The influence of binder chemical composition on acid resistance is evaluated through cumulative and differential ANC analysis, offering a rapid and novel approach to assess the durability of geopolymers in low pH environments.

2 Materials and methods

2.1 Titration setup

For the titration experiments, the titration unit utilized is a Zeta potential device called DT310, manufactured by Dispersion Technology. The device is equipped with two automatic burettes, a pH electrode, and a temperature sensor, allowing for continuous measurements. The titration unit is software-controlled and programmable to perform various protocols automatically, including dosing specific amounts of additives, acids, bases, and controlling pH values and time. A high-performance pH electrode from Metrohm, known as Unitrode glass electrode with item number 6.0259.100, is employed in the setup. To ensure proper mixing of the solution, a laboratory magnetic stirrer (Hannah Instruments, model HI 190 M) is utilized, along with a 300 ml beaker and a magnetic stirring bar. The entire experimental setup is assembled inside a fume hood (Figure 1). During the experiment, 1.5 grams of powdered cement sample is added to 150 grams of demineralized water. After allowing 5-10 minutes for the cement dissolution process to stabilize, the automatic titration process begins once the pH values reach a constant level. The device continuously measures the pH value using the following setup parameters: 100 mL of acid solution is added in 501 steps, with a tolerance of 0.05 and a drift rate of 0.0005 pH/s (or 0.001 pH/s/s). The equilibration time between each dosing step ranges from 60 seconds (minimum) to 300 seconds (maximum). Acid is dosed at each step once the pH value reaches equilibrium, indicating that only permissible fluctuations occur. This process is repeated until all 501 dosing steps are completed. The duration of each experimental run typically takes approximately one day, depending on the specific acid and type of cement being investigated.

2.2 Differential Acid Neutralization Analysis

To improve the identification of plateaus in the titration curve, a mathematical differentiation technique called Differential Acid Neutralization Analysis (dANA) was employed [4]. This mathematical treatment approach involved transposing the axes of the standard titration curve

presentation and plotting the absolute value of the slope between adjacent measured points against the corresponding pH values within that range. However, the literature is not precise enough about the required mathematical treatment, as the inversion of X and Y axis may pose challenges in making the differential curve. Thus, here we provide a procedure. After reversal of axis, the curve was smoothed (linear Savitzky–Golay using a frame length of 5 datapoints), interpolated with (300) equally spaced data points, subjected to a process of derivation, smoothed again (using linear Savitzky–Golay and a frame length of 15 datapoints), and finally multiplied by a factor of $-1/1.5$ (-1 due to axis inversion and divided by 1.5 g of binder powder). This yields a unit of the ordinate in [mL acid solution per 1g of powdered cement], and to convert that unit into the Acid (proton) in units of mol/g, one must simply divide by 1000 (as 1 mol/L acid solution was used here). Differentiation was made by a centered difference algorithm (implemented in Origin Pro software), which calculates the derivative at each (discrete) data point by taking the average of the slopes between the point and its two closest neighbours. The data analysis can be easily automated by writing a code, e.g. in Octave/Matlab.

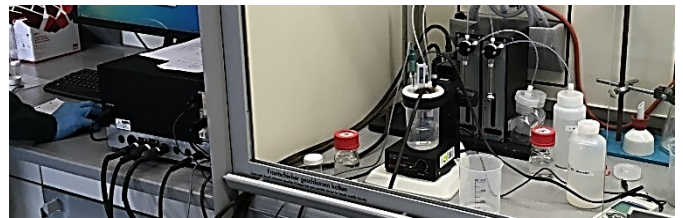


Figure 1 Automated titration experimental setup used in the study.

2.3 Materials

Two types of metakaolin were employed: a high-purity metakaolin (Mm), and a quartz-rich metakaolin (MWr). Quantitative powder X-ray diffraction analysis revealed that Mm contained 81 wt.% amorphous and 10 wt.% quartz, while MWr contained 50 wt.% amorphous and 40 wt.% quartz. The Blaine specific surface areas are 26,000 cm²/g (median grain size of 6 μm) and 10,000 cm²/g (median grain size of 41 μm), respectively. The alkaline activator used was a potassium silicate solution (Woellner GEosil 14517) with a molar SiO₂/K₂O ratio of 1.7, solid content of approx. 45.0 %, density (20°C) of approx. 1.5 g/cm³, pH (20°C) approx. 12.5 and viscosity (20°C) of approx. 20 mPas. Calculated chemical composition (based on the given molar ratio and solid content) is 23.4 mass % SiO₂ and 21.6 mass % K₂O. Geopolymer pastes were prepared with a metakaolin-to-waterglass mass ratio of 2 for Mm and 0.8 for MWr. For Portland cement (CEM I 42,5 R) and CAC a water-to-cement ratio of 0.5 was used. Main mineral phase in CAC is CA (minor: C₂AS, CT, C₁₂A₇); nominal chemical composition: Al₂O₃ 50–53, CaO ≤ 40, SiO₂ ≤ 6, Fe₂O₃ ≤ 3.0, MgO ≤ 1.5, SO₃ ≤ 0.4. After mixing, the fresh pastes were molded into 4x4x4 cm cubes and cured at room temperature for 28 days. CAC pastes underwent hydrothermal conversion, where metastable phases were transformed into stable ones. This conversion process was carried out by sealing samples with water in a jar and subjecting them to hydrothermal conditions at 70°C for 1 day.

The two acids employed in the titration are acetic acid and hydrochloric acid, with a concentration of $c = 1$ mol/L.

3 Results

In Figure 2, the neutralization curves of different binder types show significant differences with increasing acid dosage. The initial pH values before acid addition already vary, with PC having the highest pH of 12.35, followed by GP_MWr (pH 11.38), CAC (pH 10.39), and GP_Mm (pH 10.0). Due to the absence of portlandite, CAC and GP have lower buffering capacities. GPs exhibit rapid pH drops due to alkalinity neutralization without significant solids dissolution, while CAC and GP_Mm have distinct plateaus around pH 4 due to alumina gel dissolution and geopolymer gel dealumination, respectively. PC shows higher pH values until crossing the CAC curve at 39 ml HCl dosage. CAC exhibits slightly better neutralization capacity at very low pH. Below pH 4, GP_Mm has higher buffering capacity than GP_MWr, consistent with the higher amount of geopolymer gel in GP_Mm.

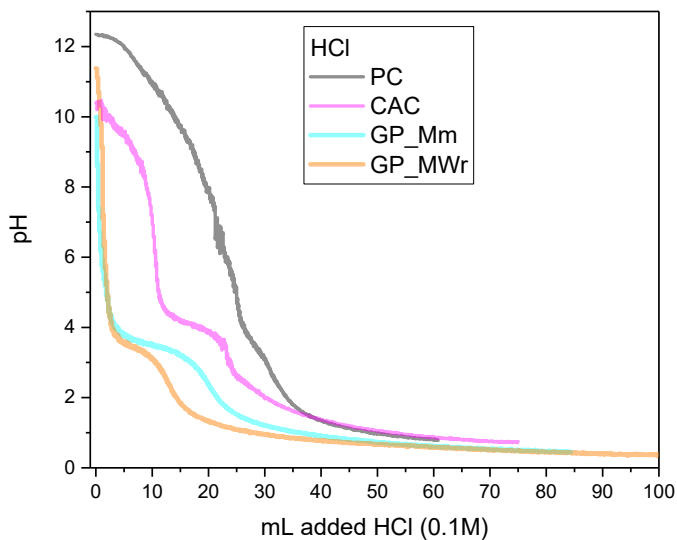


Figure 2 Neutralization of the different binders due to titration with acetic acid.

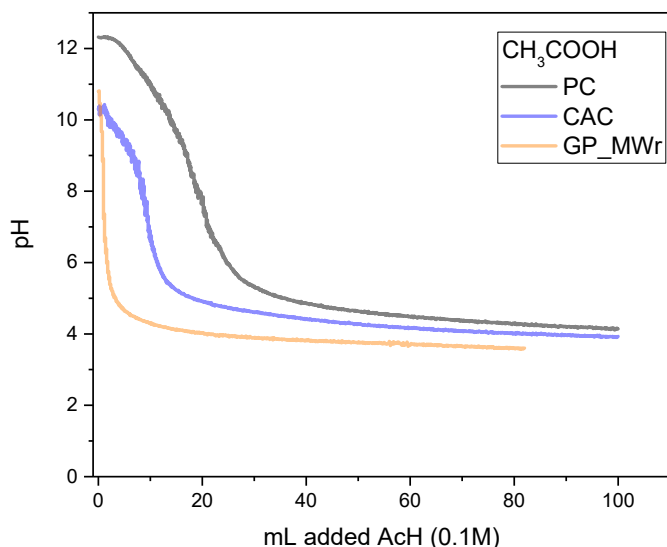


Figure 3 Neutralization of the binders by titration with acetic acid.

Figure 3 shows the pH titration curves of different hydrated binders (PC, CAC, and GP_MWr) when exposed to acetic acid. The initial pH values before acid addition are already distinct, with PC having the highest pH of 12.32, followed by GP_MWr (pH 10.8) and CAC (pH 10.4). The absence of

portlandite in CAC and GP results in lower buffering capacity. GP shows a steep neutralization curve as it primarily neutralizes the alkalinity of the solution through alkali ion exchange, without significant solid dissolution. After an initial pH overlap, the curves diverge, reaching different pH values. At an acid dosage of 80 ml, the pH values are 4.3 (PC), 4.0 (CAC), and 3.6 (GP_MWr). PC and CAC exhibit a flat region indicating higher buffering capacity, followed by a rapid pH decline after depletion of calcium hydroxide or C3AH6 phases. This decline follows a typical 'S-type' multi-decay curve, eventually leveling off.

The results on the effect of acid type, acetic vs. HCl, are discussed next by comparing Fig 3. and 4. The initial pH values for both experiments show no significant differences. HCl as a strong acid that is fully dissociated, has all protons, 1 mol/L, available for direct neutralization. On the other hand, acetic acid is only partially dissociated, resulting in initially fewer protons available for neutralization, and not being able to reach values below about pH 4. Complexation effects of the metal-acetates could be another important parameter for the solubility of phases, e.g. rich in Ca and Al (and Fe). Due to the difference in acid dissociation strength (weak in acetic and strong in HCl), different pH values are reached at the end of the titration experiments. For acetic acid, it is suspected that limited amount of alumina hydroxide phases dissolve since the pH value in the (acetic acid) experiments does not reach below pH 4.0. Higher concentrations ($>>1$ mol/L) should be tested to reach lower pHs. In general, the powder residues in experiments with both acids indicate that not all phases are completely dissolved at the end. More undissolved powder was observed for geopolymer samples.

4 Discussion

The lower buffering capacity (around pH 4, Fig. 2) observed in GP_MWr, as compared to GP_Mm, can be attributed to differences in the mix designs of the geopolymers. Specifically, the lower overall amount of reactive precursors (metakaolin and waterglass) and the lower reactive Al/Si ratio, resulting from a lower waterglass to reactive metakaolin ratio in the MWr mix, led to a reduced formation of geopolymer capable of binding alkalis within its solid framework network. This lower alkali-binding capacity allowed for higher concentrations of free alkali in the solution, resulting in higher (initial) pH. Additionally, the release kinetics of the bound alkali may not have posed a significant limitation in both GP mixes, resulting in rapid reduction of pH reaching a buffering at pH 4 due to onset of geopolymer gel dissolution.

The main hydration products found in hardened pastes of calcium aluminate cement (CAC) are hydrogarnet (C3AH6) and gibbsite (AH3 or alumina gel). If blending CAC with carbonates or silica-rich pozzolans, monocarbonate (C3ACcH11) or stratlingite (C2ASH8) may also form. However, when considering original CAC without any blending, only C3AH6 and AHx (gibbsite) are typically considered as the primary hydration products.

As a method for investigating the neutralization capacity, the titration experiments carried out here have the advantage over other methods in that they require little time. A test run requires only a day, or even only few hours.

However, 1 day is preferable to reach adequate resolution (step size dosage in mL) to make satisfactory derivative curve. The method is therefore suitable for obtaining an initial overview of the neutralization behaviour of various cement types. In other experimental methods, such as the method used by Berger et al. [9], the powdered samples are stored in the acid for more than 100 days until results are available for evaluation. These may be more accurate for this purpose, as the pH has significantly more time to approach a final value. However, the effects of carbonation are challenging to alleviate.

4.1 Differential Acid Neutralization Analysis

The differential acid neutralization analysis (dANA) plots are created from the titration curves using the method described in methodology section. These spectra are intended to provide a better interpretation of the results obtained from the titration curves. Buffer effects, which are equivalent to the slopes of the titration curves, are difficult to identify directly. However, in the dANA, these buffer effects can be observed more clearly as peaks. As a result of the dANA analysis, a series of distinct peaks were generated at the pH values corresponding to each plateau. This technique effectively enhanced the visualization and characterization (Figures 3 and 4) of the plateaus in the (integral) titration curve (Figures 1 and 2). First, a note on the unit in ordinate of Figures 4 and 5, which is in [mL acid solution per 1g of powdered sample], and to convert that unit into the Acid (proton) in units of mol/g, one has to simply divide by 1000, as 1 mol/L acid solution was used.

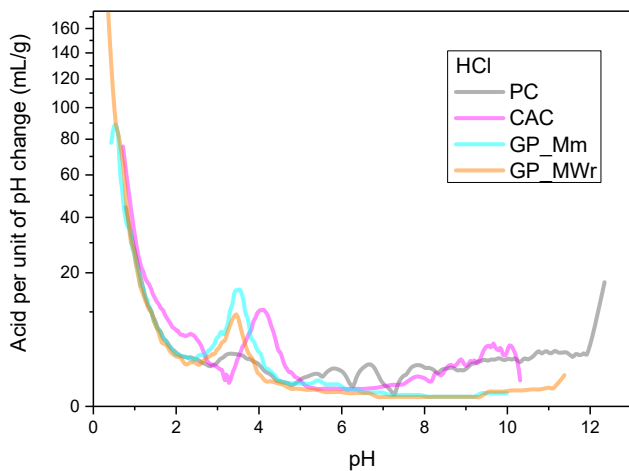


Figure 4 Differential acid neutralization analysis of HCl titration curves. For better visualization a square scale is used on ordinate. To convert the unit in ordinate into mol/g, one has to simply divide by 1000, as 1 mol/L acid solution was used.

Results of dANA for HCl acid case (Fi. 4) show differences in (buffering) peaks due to different chemistry of the binders. For PC and GP_Mwr samples, a distinct peak can be observed in the high pH range, above pH 12 (portlandite) and 11 (C₃AH₆), respectively. In literature, following pH values are found for stability of some typical phases: Calciumhydroxid (portlandite, pH = 12.6; 12.5 [10, 11]; 12,0 [6, 17]), Monosulfat (AFm, pH = 11.6 [12]; 9.0 - 10.0 [6]; Ettringit (AFt, pH = 11.0; 10.6 - 10.7 [10, 11-14]; ~ 9.0 - 10.0 [10]), Gypsum (pH = 11.6 - 10.6 [11]); C-S-H (pH = 10.5 [10]; 9.0 [17]; 8.8 [10, 11]), C₃AH₆ (pH = 10.0 [12]) and alumina gel (AH_x, pH = 3.0 - 4.0 [6]; 3.0

[15]). At even lower pH values, almost all phases are dissolved, leaving behind only an amorphous silica gel with small amounts of aluminum and iron [9, 16].

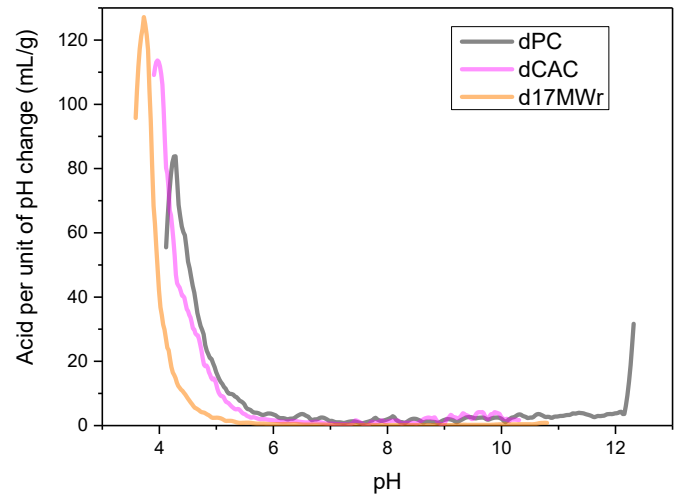


Figure 5 Differential analysis of the acetic acid titration.

Table 1 provides an overview of the chemical acid-base neutralization reactions of geopolymer binders in comparison to conventional cement-based binders (PC and CAC).

Table 1 Comparison of Compositional Changes and Dissolution Behavior of Geopolymer, Calcium Aluminate, and Portland Cements under Acetic and HCl Acid Attack. Cement chemistry notation (C-CaO, A-Al₂O₃, H-H₂O, S-SiO₂) is used.

Solubility	GP low Ca high Si & Al	CAC low Si high Ca &	PC low Al high Ca & Si
High	K ⁺ /Na ⁺ from K-A-S-H gel	C ₃ AH ₆ ; (CAH ₁₀ , C ₂ A(S)H ₈)	CH; Ca from C-S-H gel
Medium	Al from A-S- H gel	A-H gel; (AH ₃)	(A-H gel)
Low	S-H gel	(S-H gel)	S-H gel

Geopolymers, as alkali-activated binders, exhibit different chemical resistance compared to cement-based materials like Calcium Aluminate (CAC) and Portland Cement (PC). Geopolymers are primarily affected by alkali leaching and dissolution of the geopolymer alkali-alumino-silicate gel, while cement-based materials rely on the dissolution of their calcium-rich hydration products. In acid attack, conventional cement materials experience significant deterioration due to the preferential dissolution of the calcium-rich hydration products (and re-precipitation of expansive acid salts, e.g. calcium-sulfates). Alkali activated materials with higher calcium content resemble a hybrid of PC and geopolymers, offering both higher neutralization capacity and phase stability. Geopolymers are promising for acid and sulfate-resistant coatings but have limitations regarding chloride ingress and structural applications due to their more connected pore structure. The durability of CAC is attributed to lower solubility of alumina-rich products and pore-filling precipitation of secondary alumina gel. Blended PC enhances solubility by reducing portlandite content. In concrete design, regardless of the binder type, sand and

(soluble, calcitic) aggregates also play a crucial role in neutralization capacity, as well as in diffusive properties.

5 Conclusion

- The ANC test setup uses an auto-titrator to generate high-resolution titration curves. It assesses the effect of geopolymer and (PC vs. CAC) cement composition on acid resistance through cumulative and differential ANC analysis. This approach provides a rapid method to evaluate geopolymer durability in low pH environments.
- The neutralization capacity of GP is distinct from PC and CAC due to the complete dissolution of cement hydrates, such as Portlandite ($\text{Ca}(\text{OH})_2$) and C-S-H for PC, and C3AH6 for CAC, during initial reactions at $\text{pH} > 4$. Although GPs have a lower initial neutralization capacity, they buffer the pH in the range of approximately 4–2 through the dissolution of geopolymer gel (and alumina gel in CAC), leading to a higher neutralization capacity within that pH range.
- GP_MWr has lower buffering capacity (below $\text{pH} 4$) than GP_Mm due to fewer reactive precursors and a lower reactive Al/Si ratio, resulting in reduced alkali-binding geopolymer formation. The higher concentrations of free alkali in GP_MWr lead to an elevated starting pH. Acid titration rapidly decreases the pH until it reaches $\text{pH} 4$, while GP_Mm exhibits better buffering due to the partial dissolution of a higher amount of geopolymer.

Acknowledgement. This research was funded by the National German DFG organization under project number 426807554 titled “Experimentally supported multi-scale Reactive Transport modelling of cementitious materials under Acid attack (ExpeRTa)”.

Author contribution. N. Ukrainczyk: Conceptualization, Writing, Investigation, Visualisation. E. Koenders: Resources.

6 References

- [1] Ukrainczyk, N. (2021) *Simple Model for Alkali Leaching from Geopolymers: Effects of Raw Materials and Acetic Acid Concentration on Apparent Diffusion Coefficient*. *Materials* 14, no. 6, 1425. <https://doi.org/10.3390/ma14061425>
- [2] Wahlström M, Laine-Ylijoki J, Kaartinen T, Ole Hjelm och David Bendz. Acid neutralization capacity of waste - specification of requirement stated in landfill regulations. Copenhagen: Nordic Council of Ministers 2009.
- [3] Stegemann JA, Shi C. (1997) *Acid Resistance of Different Monolithic Binders and Solidified Wastes*. *Studies in Environmental Science* 71, 551–562. [https://doi.org/10.1016/S0166-1116\(97\)80238-5](https://doi.org/10.1016/S0166-1116(97)80238-5)
- [4] Glass GK, Buenfeld NR. Differential acid neutralisation analysis. *Cement and Concrete Research* 1999; 29(10): 1681–4. [https://doi.org/10.1016/S0008-8846\(99\)00127-1](https://doi.org/10.1016/S0008-8846(99)00127-1)
- [5] Glass, G.K., Reddy, B., Buenfeld, N.R. (2000) *Corrosion inhibition in concrete arising from its acid neutralisation capacity*. *Corrosion Science* 42, 1587–1598. [https://doi.org/10.1016/S0010-938X\(00\)00008-1](https://doi.org/10.1016/S0010-938X(00)00008-1)
- [6] Damion, T., Chaunsali P. (2022) *Evaluating acid resistance of Portland cement, calcium aluminate cement, and calcium sulfoaluminate based cement using acid neutralisation*. *Cement and Concrete Research* 162, 107000. <https://doi.org/10.1016/j.cemconres.2022.107000>
- [7] Mellado, A., Pérez-Ramos, M.I., Monzó, J., Borrachero, M.V., Payá J. (2017) *Resistance to acid attack of alkali-activated binders: Simple new techniques to measure susceptibility*. *Construction and Building Materials* 150, 355–366. <http://dx.doi.org/10.1016/j.conbuildmat.2017.05.224>
- [8] Koenig, A., Herrmann, A., Overmann, S., Dehn, F. (2017) Resistance of alkali-activated binders to organic acid attack: Assessment of evaluation criteria and damage mechanisms. *Construction and Building Materials* 151,405–413. <https://doi.org/10.1016/j.conbuildmat.2017.06.117>
- [9] Berger, F., Bogner, A., Hirsch, A., Ukrainczyk, N., Dehn, F. and Koenders E. (2022) *Thermodynamic Modeling and Experimental Validation of Acetic Acid Attack on Hardened Cement Paste: Effect of Silica Fume*. *Materials* 15, no. 23, 8355. <https://doi.org/10.3390/ma15238355>
- [10] Beddoe RE, Dorner HW. (2005) *Modelling acid attack on concrete: Part I. The essential mechanisms*. *Cement and Concrete Research* 35(12), 2333–9. <https://doi.org/10.1016/j.cemconres.2005.04.002>
- [11] Reardon, E.J. (1989) *An ion interaction model for the determination of chemical equilibria in cement/water systems*. *Cement and Concrete Research* 20, 175–92.
- [12] Gabrisova A.JH. (1991) *Stability of calcium sulphoaluminate hydrates in water solutions with various pH values*. *Cement and Concrete Research* 21, 1023–1027. [https://doi.org/10.1016/0008-8846\(91\)90062-M](https://doi.org/10.1016/0008-8846(91)90062-M)
- [13] McCarthy, G.J., Hassett, D.J. & Bender, J.A. (1991) *Synthesis, Crystal Chemistry and Stability of Ettringite, A Material with Potential Applications in Hazardous Waste Immobilization*. *MRS Online Proceedings Library* 245, 129–140. <https://doi.org/10.1557/PROC-245-129>
- [14] Myneni, S. (1998) *Ettringite solubility and geochemistry of the $\text{Ca}(\text{OH})_2\text{-Al}_2(\text{SO}_4)_3\text{-H}_2\text{O}$ system at 1 atm pressure and 298 K*. *Chemical Geology* 148, 1–19.
- [15] Pavlik V. (1994) *Corrosion of hardened cement paste by acetic and nitric acids: Part II: formation and chemical composition of the corrosion products layer*. *Cement and Concrete Research* 24(8), 1495–1508.

- [16] Bertron A, Duchesne J, Escadeillas G. (2005) *Attack of cement pastes exposed to organic acids in manure*. *Cement and Concrete Composites* 27(9-10), 898–909. <https://doi.org/10.1016/j.cemconcomp.2005.06.003>
- [17] Shi C, Stegemann JA. (2000) *Acid corrosion resistance of different cementing materials*. *Cement and Concrete Research* 30(5), 803–8. [https://doi.org/10.1016/S0008-8846\(00\)00234-9](https://doi.org/10.1016/S0008-8846(00)00234-9)